Electrochemical Rectification by Redox-Labeled Bioconjugates: Molecular Building Blocks for the Construction of Biodiodes

Omar Azzaroni,*,† Mònica Mir,† Marta Álvarez,† Louis Tiefenauer,‡ and Wolfgang Knoll†

Max-Planck-Institut für Polymerforschung, Ackermannweg 10, 55128, Mainz, Germany, and Life Sciences Department, Paul Scherrer Institute, CH 5232 PSI, Villigen, Switzerland

Received November 13, 2007. In Final Form: December 2, 2007

In the present work, we describe the properties of a bifunctional redox-labeled bioconjugate at electrode surfaces mediating the electron transfer across the electrode−electrolyte interface. We show that the assembly of ferrocene-labeled streptavidin on biotinylated electrodes results in a reproducible unidirectional current flow in the presence of electron donors in solution. Such rectifying films were built up by spontaneous binding of tetrameric streptavidin molecules to biotin centers immobilized on the electrode surface. Due to the high affinitiy of biotin to streptavidin, such bifunctional films completely bind any biotinylated compounds. The charge transport between donors in solution and the Au electrode is mediated by the ferrocene moieties, allowing us to develop a molecular rectifier. Our experimental results suggest that such redox-labeled proteins with a high binding capacity constitute a promising alternative to organic compounds used in molecular electronics.

Introduction

Gaining control over the electron transport at solid−liquid interfaces is of mandatory importance in different research fields.[1] Tailoring electrode surfaces to control the electron transport has become the bedrock of the new biosensing strategies.[2] As in molecular electronics, assemblies of molecules are commonly used to produce switches and storage devices of nanosized dimensions.[3,4]

Within this ever growing research field, electrochemistry played a key role to develop simple and reliable procedures to control the charge transfer across interfaces.[5−12] It is worth noting that supramolecular and macromolecular chemistry has contributed significantly to these electrochemical approaches by providing tailor-made compounds for the molecular design of electrode surfaces.[13−18] The pioneering and inspiring works from the groups of Murray[19−21] and Wrighton[22−24] paved the way to use organic thin films for controlling the charge transfer at electrochemical interfaces. These strategies were mostly based on using molecular assemblies containing redox centers[25,26] to tailor the electron transfer at the metal/electrolyte interface in order to achieve current rectification. It became evident that molecular modification of the electrode surface can lead to drastic changes in the electronic readout, i.e., unidirectional current flow or so-called diode-like behavior.

When thin polymer films are used to build up diodelike interfaces for current rectification, the presence of defects in the organic layer[27] are mainly responsible for the current leakage. Therefore, it is of particular interest to explore alternatives and new strategies to obtain such rectifying films exhibiting sufficiently high blocking characteristics and fast electron-transfer kinetics. Mixed redox-labeled dendrimers and alkanethiolate monolayers have been investigated in this respect. Crooks and co-workers were able to design excellent thin rectifying films by exploiting the unique properties of dendrimers.[27] In a similar way, proteins have been demonstrated to be exquisite building blocks to create nanosystems at interfaces[28,29] which form spatially ordered structures retaining their unique binding capacity.

* To whom correspondence should be addressed. Phone: +49-6131-379357. Fax: +49-6131-379330. E-mail: azzaroni@mpip-mainz.mpg.de.

† Max-Planck-Institut für Polymerforschung.

‡ Paul Scherrer Institute.

(1) Adams, D. M.; Brus, L.; Chidsey, C. E. D.; Creager, S.; Creutz, C.; Kagan, C. R.; Kamat, P. V.; Lieberman, M.; Lindsay, S.; Marcus, R. A.; Metzger, R. M.; Michel-Beyerle, M. E.; Miller, J. R.; Newton, M. D.; Rolison, D. R.; Sankey, O.; Schanze, K. S.; Yardley, J.; Zhu, X. *J. Phys. Chem. B* **2003**, *107*, 6668−6697.

(2) Katz, E.; Shipway, A. N.; Willner, I. In *Bioelectrochemistry*; Bard, A. J., Stratmann, M., Willson, G. S., Eds.; VCH-Wiley: Weinheim, 2002; Chapter 17, p 559.

(3) Balzani, V.; Venturi, M.; Credi, A. *Molecular Devices and Machines: A Journey to the Nanoworld;* VCH-Wiley: Weinheim, 2003.

(4) Tseng, H. R.; Celestre, P. C.; Stoddart, J. F. In *Macromolecular Nanostructured Materials;* Ueyama, N., Harada, A., Eds.; Kodansha Ltd.: Tokyo, 2004; Chapter 1.1, pp 2−25.

(5) Sabatani, E.; Anson, F. C. *J. Phys. Chem.* **1993**, *97*, 10158−10165.

(6) McCoy, C. H.; Wrighton, M. S. *Chem. Mater.* **1993**, *5*, 914−916.

(7) Han, D. X.; Shimada, S.; Murray, R. W.; Silver, M. *Phys. Rev. B* **1992**, *45*, 9436−9438.

(8) Shigehara, K.; Oyama, N.; Anson, F. C. *J. Am. Chem. Soc.* **1981**, *103*, 2552−2558.

(9) Chii, Q.; Zhang, J.; Ulstrup, J. *J. Phys. Chem. B* **2006**, *110*, 1102.

(10) Berchams, S.; Usha, S.; Ramalechume, C.; Yegnaraman, J. *Solid State Electrochem.* **2005**, *9*, 595.

(11) Maksymiuk, K.; Doblhofer, K. *Electrochim. Acta* **1994**, *39*, 217−227.

(12) Doblhofer, K.; Armstrong, M. D. *Electrochim. Acta* **1988**, *33*, 453−460.

(13) Hempenius, M. A.; Robins, N. S.; Peter, M.; Kooij, E. S.; Vancso, G. J. *Langmuir* **2002**, *18*, 7629−7634.

(14) Peter, M.; Lammertink, R. G. H.; Hempenius, M. A.; Vancso, G. J. *Langmuir* **2005**, *21*, 5115−5123.

(15) Zou, S.; Ma, Y.; Hempenius, M. A.; Schonherr, H.; Vancso, G. J. *Langmuir* **2004**, *20*, 6278−6287.

(16) Auletta, T.; van Veggel, F. C. J. M.; Reinhoudt, D. N. *Langmuir* **2002**; *18*, 1288−1293.

(17) Kaifer, A. E.; Gómez-Kaifer, M. In *Supramolecular Electrochemistry;* VCH-Wiley: Weinheim, 2000.

(18) Castro, R.; Cuadrado, I.; Alonso, B.; Casado, C. M.; Moran, M.; Kaifer, A. E. *J. Am. Chem. Soc.* **1997**, *119*, 5760−5761.

(19) Murray, R. W. *Phil. Trans. R. Soc. A: Math. Phys. Eng. Sci.* **1981**, *302*, 253−265.

(20) Murray, R. W. In *Electroanalytical Chemistry;* Bard, A. J., Ed.; Marcel Dekker: New York, 1984; Vol. 13, pp 191−368.

(21) Chidsey, C. E. D.; Murray, R. W. *Science* **1986**, *231*, 25.

(22) Palmore, G. T. R.; Smith, D. K.; Wrighton, M. S. *J. Phys. Chem. B* **1997**, *101*, 2437−2450.

(23) Smith, D. K.; Lane, G. A.; Wrighton, M. S. *J. Am. Chem. Soc.* **1986**, *108*, 3522−3525.

(24) Wrighton, M. S. *Science* **1986**, *231*, 32.

(25) Lyons, M. E. G. In *Electroactive Polymer Electrochemistry Part 1: Fundamentals;* Lyons, M. E. G., Ed.; Plenum Press: New York, 1994; Chapter 1, p 1.

(26) Majda, M. *Molecular Design of Electrode Surfaces*; Murray, R. W., Ed.; Wiley: New York, 1992; Chapter 4, p 159.

(27) Oh, S. K.; Baker, L. A.; Crooks, R. M. *Langmuir* **2002**, *18*, 6981.

(28) Niemeyer, C. M. In *Nanobiotechnology: Concepts, Applications and Perspectives;* Niemeyer, C. M., Mirkin, C. A., Eds.; VCH-Wiley: Wienheim, 2004; Chapter 15, p 227.

10.1021/la703536a CCC: $40.75
Published on Web 02/01/2008

In the present work, we used ferrocene-labeled streptavidin conjugates at electrochemical interfaces to achieve reproducible unidirectional current flow. The robust rectifying films were formed by the spontaneous and strong binding of the bioconjugates (as molecular building blocks) to biotin moieties immobilized on the electrodes. Our findings demonstrate that such redox-labeled proteins with a high binding capacity are suitable to build up functional electrochemical interfaces.

Experimental Section

Materials: Streptavidin (SAv), potassium ferrocyanide, phosphate-buffered saline (PBS), *N*-hydroxysuccinimide (NHS), dimethylformamide (DMF), [*N*-(3-dimethylaminopropyl)-*N*′-ethylcarbodiimide hydrochloride] (EDC), and 11-mercaptoundecanol were purchased from Sigma-Aldrich. Biotin-terminated thiol [**1**, 12-mercaptododecanoic-(8-biotinoylamido-3,6-dioxaoctyl)amide] was obtained from Boeringer Mannheim. [*N*-(Ferrocenylmethyl)-6-amino)hexanoic acid was synthesized as previously described in the literature.[30]

Synthesis of Ferrocene-Labeled Streptavidin (Fc−SAv). [*N*-(Ferrocenylmethyl)-6-amino)hexanoic acid (30 mg, 91 μmol), *N*-hydroxysuccinimide (11 mg, 96 μmol), and [*N*-(3-dimethylaminopropyl)-*N*′-ethylcarbodiimide hydrochloride] (18 mg, 94 μmol) in 0.5 mL of dry DMF were heated under N_2 amosphere and stirring at 80 °C for 30 min. Aliquots (5×10 μL) of these solutions were added at room temperature to a solution of 1 mg of streptavidin in 0.5 mL of phosphate buffer (0.1 M, pH 8.5). To remove unreacted ferrocene, the solution of the modified streptavidin was extensively dialyzed against PBS buffer (0.05 M, pH 7.4). The spectrophotometrically determined Fc/SAv ratio was ∼14. The biotin binding capacity of Fc−SAv was determined in a competitive assay and was found to be similar to that of SAv.[31,32]

Electrochemical Measurements. Cyclic voltammetry experiments were performed with an Autolab potentiostat using a conventional three-electrode cell equipped with an Ag/AgCl reference electrode and a graphite counter electrode.

Surface Plasmon Resonance. Surface plasmon resonance (SPR) detection was carried out in a homemade device under a Kretschmann configuration.[33] The SPR substrates were a BK7 glass coated with 2 nm of chromium and 50 nm of gold by evaporation. The substrate was incubated overnight with a mixture 1:9 of biotin-terminated thiol and 11-mercapto-1-undecanol. Afterward, the surface was rinsed with ethanol and dried with N_2 followed by 2 h of streptavidin incubation in 0.1 M PBS buffer. The same buffer was used to rinse the biomolecules that were not bound to the biotinylated surface. Before and after streptavidin conjugate injection a measure of SPR signal at different angles was recorded to detect the shift of the minimum angle of reflectance due to the streptavidin immobilization on the surface. The SPR angle shifts were converted into mass uptakes using the experimentally determined relationship, Γ (ng mm^{-2}) = $\Delta\theta$ (deg)/0.19. The sensitivity factor was obtained following procedures reported in the literature.[34]

SPR was also used to determine the equivalent thickness of the bioconjugate film. The procedure has been described in detail elsewhere.[33] The equivalent thickness of the SAv layer was calculated from the SPR optical thickness (*nd*) measured prior to and after Fc−SAv bioconjugation, assuming a refractive index *n* of 1.42 for the protein layer.

Atomic Force Microscopy: Images were taken in air at room temperature with a commercial AFM Dimension 3000 (Veeco) controlled with a Nanoscope V, operating in tapping mode. Silicon cantilevers (Olympus) 160 μm long, 50 μm wide, and 4.6 μm thick, with an integrated tip of a nominal spring constant of 42 N/m and a resonance frequency of 300 kHz, were used. In a typical experiment, the tip was scanned at velocity in the range 0.8−1 Hz, and minimal applied forces were used when imaging. Topography and phase images were used to record the structures. Samples for AFM analysis were prepared by immersing freshly prepared gold-coated ultraflat mica surfaces in the mixed thiol solution overnight. After careful rinsing with ethanol, the biotinylated substrates were incubated for 2 h with a 200 nM Fc−SAv in 0.1 M PBS buffer. The samples were then rinsed with water, dried with nitrogen, and shielded from dust particles.

Results and Discussion

A self-assembled monolayer (SAM) is chemisorbed on Au electrodes (Figure 1) using 12-mercaptododecanoic-(8-biotinoylamido-3,6-dioxaoctyl)amide (**1**) and 11-mercapto-1-undecanol in a 1:9 ratio. This mixture leads to a density of biotin moieties which best binds SAv conjugates as reported by Spinke et al.[36] and López and co-workers.[37] Stayton et al.[38] have recently reported in a systematic study that the surface density of SAv bound to a mixed monolayer of thiolated compounds is correlated to the molar fraction of biotin derivative in solution and that the immobilized biotin moieties were randomly distributed within the film. Therefore, we can assume that the conjugate film of our preparations is densely packed and 10% of the thiolated molecules carry a biotin moiety. The surface density of biotin is an important issue. At a higher surface density of biotin moieties, the SAv surface density will decrease due the hindered access of the recognized biotin moiety to the biotin-binding pocket of SAv.[36,37]

In order to achieve the final bifunctional surface, the biotinylated platform was incubated with 200 nM Fc−SAv in PBS buffer (Figure 1). Each SAv molecule is labeled on average with 14 ferrocene moieties through 1−1.5 nm long spacers.[30] Binding of streptavidin to biotin is one of the strongest noncovalent interaction in nature ($K = 10^{15}$ L mol^{-1}).[39] Immobilization of Fc−SAv led to a thin (∼3.5 nm), but compact bioconjugate film. Surface plasmon resonance measurements (Figure 2) of the biotinylated gold surface prior to and after incubation evidenced a well-defined shift from 56.61° to 56.74° in the minimum of the angular θ-scans of reflected intensity. This $\Delta\theta$ is related to a mass uptake that corresponds to a coverage of 7.2×10^{11} Fc−SAv molecules/cm^2.

Atomic force microscopy (AFM) imaging on the biotinylated Au electrodes also evidenced changes on the topography upon conjugate binding (Figure 3a,b). After incubation, a homogenously distributed nodular-like film is deposited on the Au electrode (Figure 3b). Determination of the height of immobilized molecules is difficult.[40] Soft proteins are usually compressed by the AFM tip, even when working at a very low applied force. As a consequence, the observed height (2−2.5 nm) is less than expected from the crystal structure (4.5 nm).[41b]

(29) Anicet, N.; Anne, A.; Moireaux, J.; Savéant, J. *Am. Chem. Soc.* **1998**, *120*, 7115.
(30) Padeste, C.; Grubelnik, A.; Tiefenauer, L. *Biosens. Bioelectron.* **2003**, *19*, 239.
(31) Padeste, C.; Steiger, B.; Grubelnik, A.; Tiefenauer, L.; *Biosens. Bioelectron.* **2004**, *20*, 545.
(32) Steiger, B.; Padeste, C.; Grubelnik, A.; Tiefenauer, L. *Electrochim. Acta* **2003**, *48*, 761.
(33) Knoll, W. *Annu. Rev. Phys. Chem.* **1998**, *49*, 569.
(34) (a) Stenberg, E.; Persson, B.; Roos, H.; Urbaniczky, C. *J. Colloid Interface Sci.* **1991**, *143*, 513−526. (b) Yu, F. Ph.D. Thesis, Johannes Gutenberg−Universität Mainz (Germany) http://www.mpip-mainz.mpg.de/knoll/publications/thesis/yu_2004.pdf.
(35) Liebermann, T.; Knoll, W.; Sluka, P.; Herrmann, R. *Colloids Surf. A* **2000**, *169*, 337−350.
(36) Spinke, J.; Liley, M.; Schmitt, F.-J.; Guder, H.-J.; Angermaier, L.; Knoll, W. *J. Chem. Phys.* **1993**, *99*, 7012−7019.
(37) Pérez-Luna, V. H.; O'Brien, M. J.; Opperman, K. A.; Hampton, P. D.; López, G. P.; Klumb, L. A.; Stayton, P. S. *J. Am. Chem. Soc.* **1999**, *121*, 6469−6478.
(38) Nelson, K. E.; Gamble, L.; Jung, L. S.; Boeckl, M. S.; Naeemi, E.; Gollegde, S. L.; Sasaki, T.; Castner, D. G.; Campbell, C. T.; Stayton, P. S. *Langmuir* **2001**, *17*, 2807−2816.
(39) Häussling, L.; Michel, B.; Ringsdorf, H.; Rohrer, H. *Angew. Chem., Int. Ed.* **1991**, *30*, 569−572.

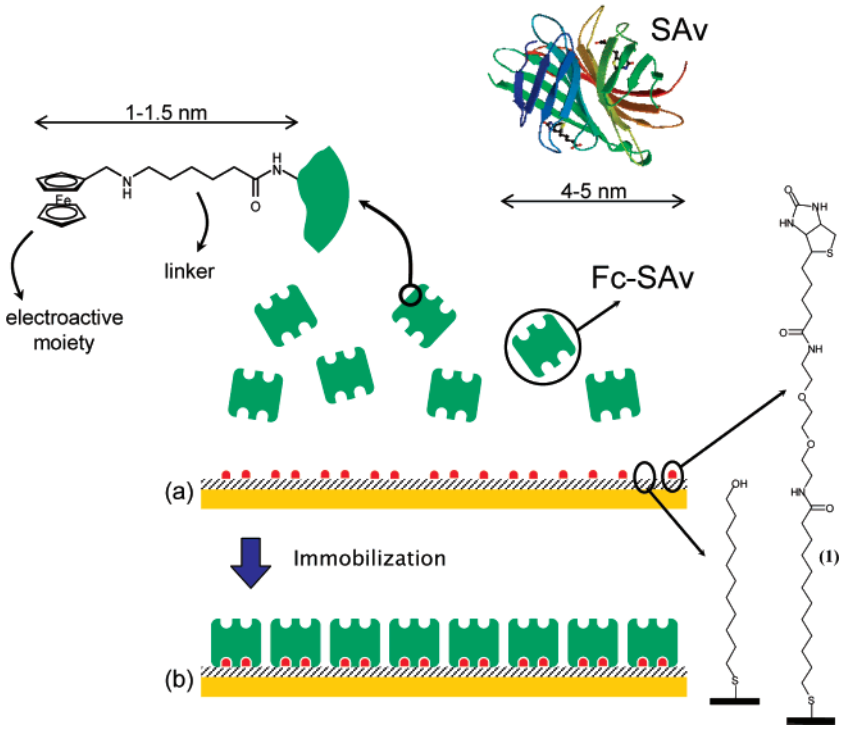

Figure 1. Simplified scheme describing the supramolecular assembly of the ferrocene-labeled streptavidin to the biotinylated Au electrode. The chemical structures of the ferrocene linker and the thiols used in this work are shown.

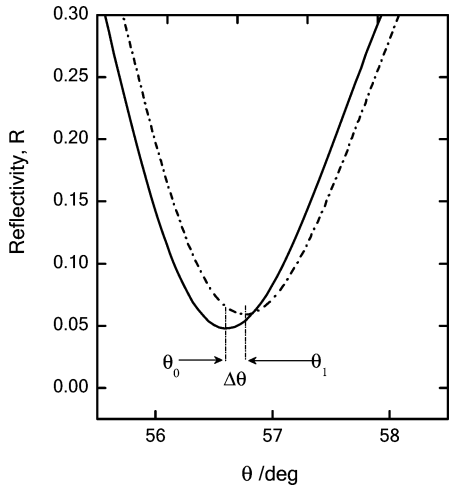

Figure 2. Reflected intensity as a function of the angle-of-incidence scan (θ) for a biotinylated Au electrode before (solid line) and after (dashed line) Fc−SAv binding. In the plot, the reflectivity minima are indicated for the biotinylated Au surface before (θ_o) and after (θ_1) incubation of 200 nM Fc−SAv in 0.1 M PBS buffer at room temperature. $\Delta\theta$ is proportional to the mass of protein immobilized on the electrode surface.

Moreover, the lateral dimension of individual molecules depends on the sharpness of the AFM tip used. Conventional tips have a radius of about 30 nm and then protein molecules appear larger due to the so-called convolution effect. Nevertheless, topographic imaging provides valuable information about the distribution of protein molecules on the electrode surface. Figure 3b clearly demonstrates that the Fc−SAv molecules are evenly distributed on the biotinylated electrode, and no patches or uncoated regions are found.

Electroactivity of the Fc−SAv films was studied by cyclic voltammetry. Figure 4 shows the cyclic voltammogram of Fc−SAv bound to the biotinylated Au electrode in PBS buffer, pH 7.4, as the supporting electrolyte. The voltammogram clearly indicates that the electron transfer across the redox-labeled protein film is feasible. In other words, despite the interface being a densely packed protein conjugate, the attached ferrocene moieties are "wired" to the Au electrode. The higher double layer capacitance observed upon oxidation, as shown on the right of the voltammogram in Figure 4, is attributed to a pronounced increase of surface charge in the Fc−SAv film. The double layer capacitance of molecular organic films has been extensively studied within theoretical[42] and experimental[43] frameworks. This characteristic feature of the voltammetric response gives an indication of and provides information about the electrostatic state of the film. In general terms, the generation of charges into the surface layer leads to an increase of the double-layer capacitance.[44] In the cathodic region at pH 7.4 each SAv protein molecule carries two negative charges. This value is based on theoretical and experimental work done by Leckband and co-workers, who estimated the effective charge of the protein.[45]

Upon oxidation, 14 positive charge units are electrochemically generated on each protein. This means that to every single bioconjugate molecule positive charges will be added by oxidizing the attached ferrocene moieties, observed as an increased capacitance.

(40) (a) Hansma, H. G.; Weisenhorn, A. L.; Gould, S. A. C.; Sinsheimer, R. L.; Gaub, H. E.; Stucky, G. D.; Zaremba, C. M.; Hansma, P. K. *J. Vac. Sci. Technol. B* **1991**, *9*, 1282. (b) Wisenhorn, A. L.; Egger, M.; Ohnesorge, F.; Gould, S. A. C.; Heyn, S.-P.; Hansma, H. G.; Sinsheimer, R. L.; Gaub, H. E.; Hansma, P. K. *Langmuir* **1991**, *7*, 8. (c) Bustamante, C.; Vesenka, J.; Tang, C. L.; Rees, W.; Guthold, M.; Keller R. *Biochemistry* **1992**, *31*, 22.

(41) (a) Shu, W.; Laue, E. D.; Seshia, A. A. *Biosens. Bioelectron.* **2007**, *22*, 2003−2009. (b) Ekgasit, S.; Stengel, G.; Knoll, W. *Anal. Chem.* **2004**, *76*, 4747−4755. (c) Kossek, S.; Padeste, C.; Tiefenauer, L. X.; Siegenthaler, H. *Biosen. Bioelectron.* **1998**, *13*, 31−43.

(42) Smith, C. P.; White, H. S. *Langmuir* **1993**, *9*, 1−3.

(43) Bryant, M. A.; Crooks, R. M. *Langmuir* **1993**, *9*, 385−387.

(44) Kakiuchi, T.; Iida, M.; Imabayashi, S.-i.; Niki, K. *Langmuir* **2000**, *16*, 5397−5401.

(45) Sivasankar, S.; Subramanian, S.; Leckband, D. *Proc. Natl. Acad. Sci. U.S.A.* **1998**, *95*, 12961−12966.

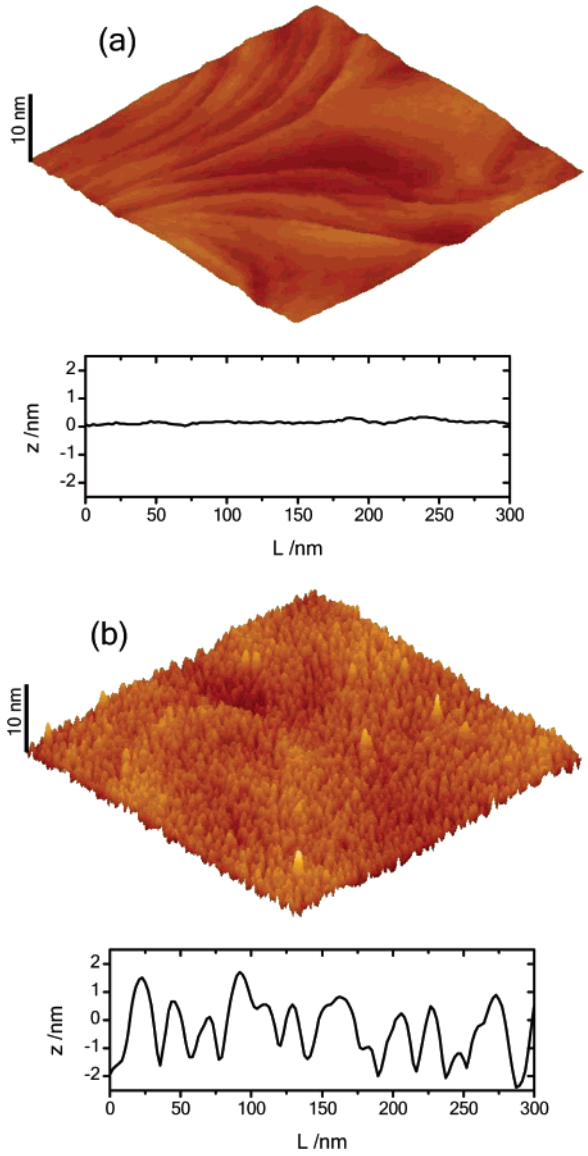

Figure 3. Atomic force microscopy images and cross-sectional analyses correspond to (a) $1 \times 1\ \mu m^2$ (3D) topographic imaging of the biotinylated SAM on gold electrode and (b) $1 \times 1\ \mu m^2$ (3D) topographic imaging of the biotinylated gold electrode after incubation with the Fc−SAv conjugate.

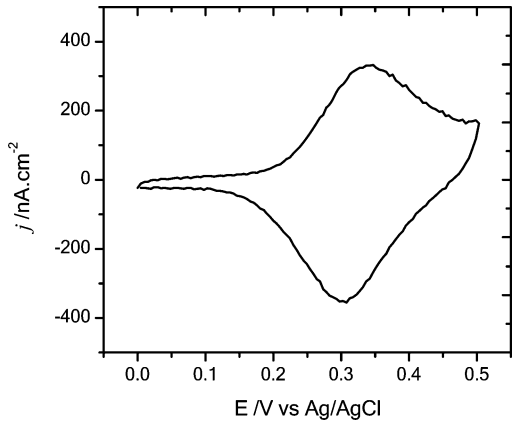

Figure 4. Cyclic voltammogram of Fc−SAv on a Au electrode in 0.1 M PBS buffer with a scans rate of 50 mV/s at 98 K.

To further explore the electrochemical characteristics of the modified electrodes, we studied voltammetric response as a function of the potential scan rate (υ). In accordance with the theory of surface-immobilized redox centers,[46] the peak current density is given by

$$j_p = \frac{n^2F^2\Gamma\upsilon}{4RT} \quad (1)$$

where n is the number of electrons involved in the electron-transfer reaction, T is the temperature, F is the Faraday constant, R is the gas constant, and Γ is the surface coverage of electroactive species.

In our experiments, the redox-labeled bioconjugate shows a linear dependence of the current density on the potential scan rate (Figure 5). These results confirm the assumption of surface-confined electroactive species of the bound conjugates. It must be noted that for a surface-confined electrochemically reversible system ΔEp should be zero.[46] In our preparation of ferrocene-labeled bioconjugates, ΔEp asymptotically tends to the minimum value of 30 mV when υ approaches zero. When υ is increased from 0.075 to 1.5 V s^{-1}, ΔEp is larger (Figure 6). This is in contrast to the findings of Steiger et al.,[32] who worked with a similar system but using a shorter cysteamine spacer for anchoring the biotin moieties to the Au electrode. This cysteamine spacer

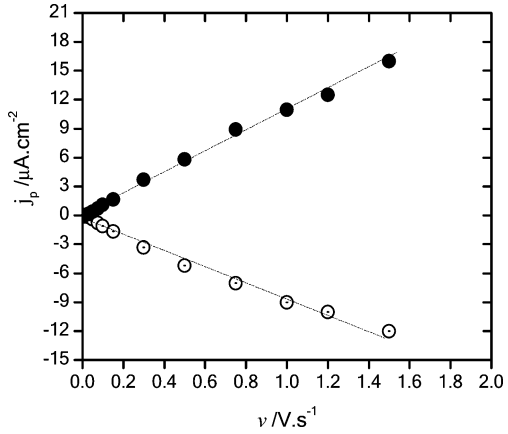

Figure 5. Representation of the peak current densities as a function of the potential scan rate. The different symbols correspond to (●) anodic peak current density and (○) cathodic peak current density. Experiments were done in 0.1 M PBS at 298 K.

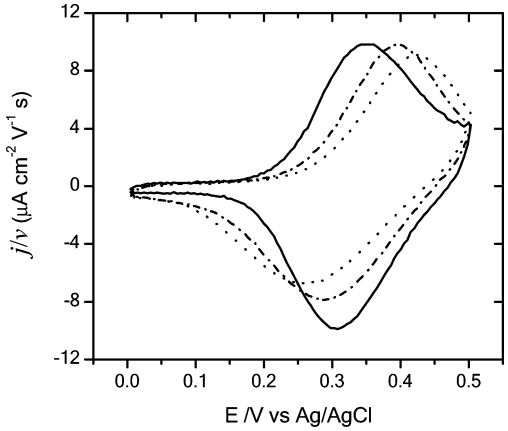

Figure 6. Cyclic voltammograms of Fc−SAv bound to a biotinylated gold electrode performed at different scan rates. The current density (j) was normalized by the potential scan rate (υ): 75 mV/s (solid line), 750 mV/s (dashed line), and 1.5 V/s (dotted line). Experiments were done in 0.1 M PBS at 298 K.

(46) Abruña, H. D. In *Electroresponsive Molecular and Polymeric Systems*; Skotheim, T. A., Ed.; Marcel Dekker: New York, 1988; Vol. 1, Chapter 3, pp 97−171.

Scheme 1

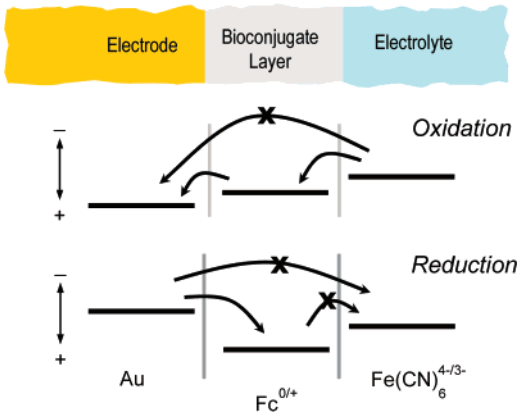

is ∼1 nm shorter than the spacer used in this study. They found no peak separation even at very high scan rates. Thus, an increase in distance of the conjugates from the electrode in the range of about 1 nm is critical. This longer linker for biotin immobilization is probably required to realize a rectifier function, as shown below.

The charge associated with these redox sites is 1.3 ± 0.2 μC/cm^{-2}, which is equivalent to ∼10^{13} ferrocene moieties per cm^2. As discussed above, the coverage of Fc−SAv is 7.2 × 10^{11} molecules/cm^2. Considering that each SAv molecule is labeled on average with ∼14 ferrocene moieties, the actual density of redox centers on the electrode surface should be 10^{13} centers/cm^2, which is in excellent agreement with the electrochemical data. The agreement of the results from electrochemical and SPR measurements strongly supports the assumption that all the redox centers linked to the streptavidin are "wired" to the Au electrode surface.

The chemical/electrochemical state of these ferrocene redox sites incorporated in the protein layer can easily be controlled by the electrode potential. As a consequence, by tuning the Fermi level of the metal electrode, i.e., controlling the electrode potential, it should be possible to transfer electrons to/from the redox labels. This means that turning the ferrocene moieties into ferricenium species can be easily controlled. However, electron donors in the solution with access to these ferricenium centers (most probably at the electrolyte site of the SAv layer) could lead to reduction of acceptor species closer to the electrode (Scheme 1). Considering the whole electron-transfer process, donor-to-redox center-to-metal, the charge-transfer event should be evidenced as an anodic current.[47] However, if the reverse reaction is thermodynamically restricted[47] or the transport of acceptors to the electrode is hindered,[48] the charge-transfer process would not be feasible (Scheme 1).

This is the situation in our preparations when electron acceptors in solution interact with reduced ferrocene sites of the immobilized conjugate. $[Fe(CN)_6]^{4-}$ species have a less noble character in comparison to Fc^0 species; their $E°$ are 0.358 and 0.400 V, respectively.[49] This means that ferricenium (Fc^+) will be spontaneously reduced to ferrocene (Fc^0) in the presence of ferrocyanide ($[Fe(CN)_6]^{4-}$) (thermodynamically favored process). But ferrocene moieties will not change their chemical state in the presence of ferricyanide ($[Fe(CN)_6]^{3-}$), because this is a thermodynamically restricted process. Consequently, no cathodic current is expected upon reversing the scan in the cathodic direction.

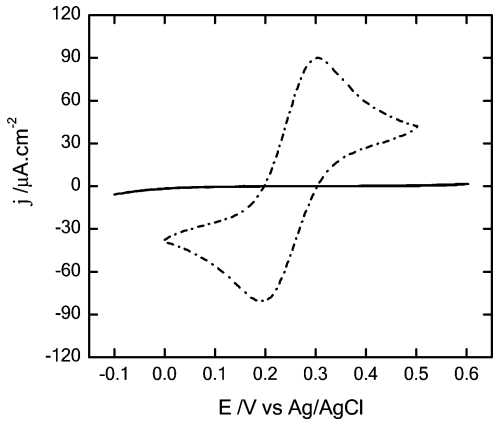

Figure 7. Voltammetric response of a bare Au electrode (dashed line) and a biotinylated Au electrode modified with nonlabeled-SAv (solid line) in a 0.1 PBS solution containing 3 mM $Fe(CN)_6^{4-}$. Experiments were done at a scan rate of 50 mV/s at 298 K.

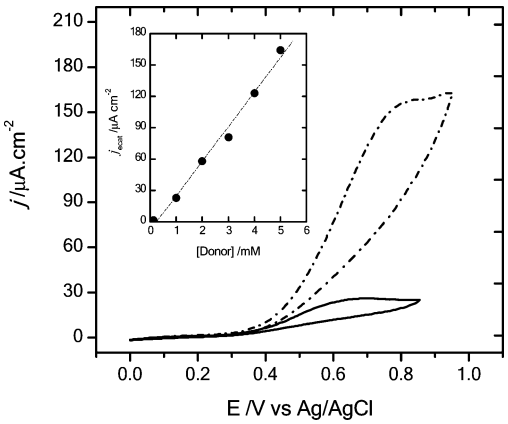

Figure 8. Cyclic voltammograms evidencing the current rectification at a biotinylated Au electrode with bound Fc−SAv. The different voltammetric scans were carried out with the same modified electrode in 0.1 M PBS buffer containing 1 mM (solid line) and 5 mM (dashed line) $Fe(CN)_6^{4-}$. The inset shows a representation of the electrocatalytic (rectified) current as a function of the concentration of donor species $[Fe(CN)_6^{4-}]$ in solution.

For probing the rectifying bioconjugate interface, the ferro/ferricyanide redox couple was used. The redox reaction of this complex is fully reversible using bare gold electrodes, whereas the reversible charge-transfer process is totally suppressed when nonlabeled SAv is bound to biotinylated Au electrode (Figure 7).

This observation indicates that, in the time scale of the experiment, redox species in solution are not able to transfer electrons to the Au surface either by approaching the electrode surface (mass transport) or by tunneling across the entire bioconjugate (charge transport).

Cyclic voltammetry of a Fc−SAv-modified Au electrode in a solution containing ferrocyanide species evidence the expected anodic peak, while no the cathodic peak is observed. More importantly, the anodic current is dependent on the concentration of donor species, as depicted in Figure 8 for 1 and 5 mM $[Fe(CN)_6]^{4-}$ solutions. It can be seen that for both concentrations the anodic current starts at about 0.37 V near the potential at which the ferrocene labels are oxidized.

This observed asymmetry of the cyclic voltammogram can be attributed to the current rectification.[27] The anodic current is

(47) Alleman, K. S.; Weber, K.; Creager, S. E. *J. Phys. Chem.* **1996**, *100*, 17050.

(48) Savéant, J. M. In *Elements of Molecular and Biomolecular Electrochemistry: An Electrochemical Approach to Electron Transfer Chemistry;* Wiley-Interscience: New York, 2006; Chapter 2, p 78.

(49) *CRC Handbook of Chemistry and Physics*; Lide, D. R., Ed.; Taylor & Francis Group: Boca Raton, FL, 2006; pp 8−20.

originated from ferrocyanide oxidation mediated by ferrocene/ferricenium species. Electron transfer is intitiated by the electrocatalytic current originated from the ferricenium reduction by ferrocyanide in solution. The correlation of the anodic peak current with the concentration of $Fe(CN)_6^{4-}$ strongly supports this assumption. In fact, the dependence of the electrocatalytic current from donor concentration (c_D) is linear (inset, Figure 8). The origin and magnitude of the current generated at an electrode modified with redox sites that undergo bimolecular electron-transfer reactions with electron donor/acceptors in solution have been studied and interpreted by a number of research groups.[50−53] Assuming a rapid generation of active sites on the electrode, $j \propto c_D$. Surface coverage of redox species and the rate constant for the bimolecular reaction kinetics are important factors determining the correlation of the rectified current and the donor species.[53] The predicted linear relationship between j and c_D is confirmed by our experimental data.

The absence of the cathodic peak in the voltammograms is attributed to the fact that (a) the electron exchange between ferrocene and $Fe(CN)_6^{3-}$ is a thermodynamically restricted process and (b) the transport of electrogenerated ferricyanide ions to the Au interface is strongly inhibited due to the blocking properties of the bioconjugate layer. This is a very important and remarkable feature of this bioconjugate interface that allowed us to build up the rectifying interface. Permeation of donor species would be evidenced as leakage currents. Crooks and co-workers used Fc-labeled dendrimers and $Fe(CN)_6^{4-}$ species that could easily reach the electrode surface by permeation across the macromolecular film.[27] To overcome this problem, the researchers back-filled the dendrimer-coated surface with hexadecanethiol. Thus, the quality of the SAM with the integrated biotin-compounds is crucial to achieve a rectifying interface. Similarly, as in the case of dendrimers, the donor species can permeate through the protein layer. Streptavidin is a negatively charged biomolecule at physiological pH (pI 5−6) that in principle would hinder the permeation of the anionic redox species to the Au electrode. However, in spite of the compact arrays of proteins, channels are formed between them through which donor species can diffuse to the underlying biotinylated SAM or even to the Au electrode. As a consequence, short incubation times (∼2 h) during the biotinylation of the Au electrode can lead to the presence of some leakage current, probably due to the defects in the organic film. This problem can be easily overcome by extending the assembly time of the biotinylated SAM to an overnight incubation. Such a prolonged assembly time is highly recommended because it leads to a more organized monolayer,[54] thus diminishing the occurences of defects, and the resulting bioconjugate film will be suitable for electrochemical rectification.

Conclusions

In this work, we have described a new film architecture for creating rectifying interfaces. We used a ferrocene-labeled streptavidin conjugate that is bound to a biotinylated Au electrode. The very specific and strong interactions between biotin and SAv result in a densely packed film of the conjugate on the electrode surface. In spite of the electrode surface being covered by the macromolecular conjugate molecules, charge transfer across the interface is feasible and the electron transfer between the redox labels and the metal electrode is slowed down only slightly. This electroactive platform was succesfully used for mediating and rectifying the electron transfer between redox donor in solution and the Au electrode. Accordingly, this supramolecular approach provides a robust interface for unidirectional current flow with excellent performance. Finally, these results demonstrate the usefulness of these bifunctional conductive layers to build up any predefined interfacial architectures in combination with biotinylated compounds of predefined properties. We consider that such versatile biointerfaces are very attractive for many applications.

Acknowledgment. O.A. acknowledges financial support from the Alexander von Humboldt Stiftung. M.Á. thanks Junta de Comunidades de Castilla la Mancha for a postdoctoral fellowship.

LA703536A

(50) Xie, Y.; Anson, F. C. *J. Electroanal. Chem.* **1995**, *384*, 145−153.
(51) Amarasinghe, S.; Chen, T.; Moberg, P.; Paul, H. J.; Tinoco, F.; Zook, L. A.; Leddy, J. *Anal. Chim. Acta* **1995**, *307*, 227−244.
(52) Andrieux, C. P.; Dumas-Bouchiat, J. M.; Savéant, J. M. *J. Electroanal. Chem.* **1982**, *131*, 1−35.
(53) Creager, S. E.; Radford, P. T. *J. Electroanal. Chem.* **2001**, *500*, 21−29.
(54) Schwartz, D. K. *Annu. Rev. Phys. Chem.* **2001**, *52*, 107−137.